ICAS 2016
30th Congress of the International Council of the Aeronautical Sciences
DCC, Daejeon, Korea ; September 25-30, 2016

LOW ORDER MODELING OF THE UNSTEADY AND 3D EFFECTS OF CONTINUOUS WAKE FLAPPING FLIGHT

Alexander Matta and Javid Bayandor
***C*Rashworthiness for *A*erospace *S*tructures and *H*ybrids (*CRASH*) Lab**
Virginia Tech

Keywords: *Flapping Flight, Lifting Line, Dynamic Stall*

Abstract

In this paper, we discuss how to model a flapping bird like wing using a variation of lifting line theory. What sets this low order modeling approach apart from other flapping lifting line models, is its modifications to include for leading edge vortex formation, the main source of extra lift in larger birds. The model was compared with experimental results from the literature with reasonable agreement. In order to further validate this approach, the model will be compared with high order Lattice Boltzmann based CFD results.

1 Introduction

The physics of flapping flight has been a subject of interest since the inception of the field of aerodynamics. Flapping flight has been shown to be very efficient, while offering excellent flight performance at low Reynolds numbers [1]. Thus, making it a feasible flight mechanism for micro/mini air vehicles. Models, both high and low order, have been previously developed to predict the aerodynamics of a flapping wing, but most have focused on the aerodynamics of smaller fliers such as hummingbirds and insects due to the interest of funding agencies in micro air vehicles. Comparatively less attention has been given to larger flapping flyers such as soaring birds.

This paper focuses on prediction of lift and drag of such flyers by utilizing a variation of lifting line theory. Several models utilizing lifting line theory have already been developed, the most recent one by W.F. Phillips [2]. Such models however, fall short of addressing the leading edge vortex (LEV) formation, which appears to be the main source of extra lift in large flapping flyers [3]. The proposed model includes the effect of LEV by using a variation of Polhamus' suction analogy [4]. Earlier strip theories that have used this suction analogy shown good agreement with experimental results [4]. However, strip theories are not ideal for prediction of lift distribution along the longitudinal axis of the wing and may not provide representative predictions for a twisting or folding wing. It is important to note that both of these mechanisms are commonly used in large birds [5].

While higher order models provide more accurate predictions, low order models tend to offer drastically reduced computation time that, depending on the complexity of the problem investigated, can be advantageous. Flapping flight has a large number of parameters associated with it, including frequency, amplitude, and possibly asymmetry between up and down stroke time. This is not including the parameters relating to additional degrees of freedom in the wing, such as dynamic wing twist and folding. With a lengthy computation time in higher order modeling methods, performing a parametric study that examines many of the parameters concerned is only currently possible through experimentation and low order models such as the one presented in this paper.

2 Nomenclature

L_{Total}	Total lift acting perpendicular to free stream
$L_{Attached}$	Lift generated acting perpendicular to free stream from wing segment with attached flow

L_{DS}	Lift generated acting perpendicular to free stream from wing segment in dynamic stall
$(\alpha_{attached})_{max}$	Max angle of attack before static airfoil stalls (transition point into dynamic stall for oscillating airfoil)
$(\alpha_{attached})_{min}$	Minimum angle of attack before static airfoil stalls (transition point into dynamic stall for oscillating airfoil)
φ	Angle of attack of flapping axis at root of wing
$\alpha'(y)$	Relative angle of attack as a function of span (takes into account effect of wing kinematics)
α_e	Effective angle of attack (chord line angle of attack to downwash deflected freestream)
α_i	Downwash induced angle of attack
α_{L0}	Angle of Zero Lift
w_i	Downwash Velocity
$y_{Attached}$	Span location where wing transitions to dynamic stall condition
ρ	Fluid density
Q_∞	Free stream velocity
$Q'_\infty(y)$	Relative free stream velocity as a function of span location (takes into account effect of wing kinematics)
ε	Wing flapping angle
$\Gamma(y)$	Circulation around wing cross section as a function of span location
b	Span length
dF_s	Leading edge suction force of an infinitely small wing segment
n_s	Leading edge suction efficiency
D_{Total}	Total drag acting parallel to free stream
D_i	Induced drag of the entire span acting parallel to free stream
D_f	Friction drag of the entire span acting parallel to free stream
C_{df}	Friction drag coefficient
$m(y)$	Local lift slope as a function of span location
$c(y)$	Chord length as a function of span location
$\alpha_{L0}(y)$	Angle of zero lift line as a function of span location
$\gamma(y)$	Twist angle of wing chord as a function of span location
$\dot{h}(y)$	Heaving velocity
A_z	Displacement amplitude of uniformly oscillating wing
A_ε	Flapping angle amplitude
f	Flapping Frequency
k	Reduced Frequency

3 Low Order Model for Flapping Wing Aerodynamic Force Prediction

The developed model is a modification of the original lifting line theory. There are three major assumptions: first, the relative angle of attack never exceeds dynamic stall range. Lifting line theory assumes attached flow. The circulation during dynamic stall is similar to the circulation during attached flow and thus lifting line theory may be able to still approximate behavior during dynamic stall. However, as soon as the wing fully stalls, lifting line theory is no longer applicable. For birds and bird like ornithopters this assumption is reasonable, as their angle of attack usually remains within the attached flow regime. However, this model is not appropriate for insect like wings, which experience much higher angles of attack causing frequent and complex vortex shedding. This likely makes the circulation around an insect wing very dissimilar to the circulation in the attached flow condition. The

second assumption is that pitching velocity of the wing has a negligible effect on relative angle of attack. For this to be true, freestream velocity must be much greater than wing section pitching velocity × chord. The last assumption is that the wing is approximately elliptical. This is necessary to have a closed loop solution to the lifting line equation.

Total lift, given by Eq. 1, is the sum of the lift generated within the inner wing section, where flow is attached. The outer wing sections are the locations where dynamic stall may occur. Based on traditional lifting line theory, lift generated by the wet sections of the wing - where flow is attached, is given by Eq. 2.

$$L_{Total} = L_{Attached} + L_{DS} \quad (1)$$

$$L_{Attached} = 2\rho \int_0^{y_{Attached}} Q'_\infty \cos(\varepsilon)\cos(\varphi+\gamma)\Gamma\, dy \quad (2)$$

where

$$(\alpha_{attached})_{min} \leq \alpha' \leq (\alpha_{attached})_{max}$$

In this model, dynamic stall is assumed to occur when the relative angle of attack exceeds the two dimensional (2-D) static stall angle. This assumption has been used in several other strip theory models [4],[6]. Eq. 3 shows the relative wing angle of attack as a function of span location by including the effect of sectional heaving motion, as well as flapping axis angle of attack and wing twist. Eq. 4 gives the relative freestream velocity as a function of span location by including the effect of sectional heaving velocity. Two commonly studied wing motions are included in this study. However, the model is not limited to these motions. Eq. 5 underlines the sectional heaving velocity of a uniformly oscillating wing (flapping angle is not a function of time and is equal to zero), while Eq. 6 gives the heaving velocity of a flapping wing with no folding or bending. For the flapping wing the motion is assumed to be sinusoidal, which is approximately what occurs for several observed species of birds [5].

$$\alpha'(y) = \tan^{-1}\frac{\dot{h}cos(\varphi)}{\dot{h}\sin(\varphi)+Q_\infty} + \varphi + \gamma \quad (3)$$

$$Q'_\infty = \sqrt{(\dot{h}\sin(\varphi)+Q_\infty)^2 + (\dot{h}\cos(\varphi))^2} \quad (4)$$

$$\dot{h} = 2\pi f A_z sin(2\pi f t) \quad (5)$$

$$\dot{h}(y) = 2\pi f y A_\varepsilon sin(2\pi f t) \quad (6)$$

Key wing kinematic parameters and flow angles are depicted in Fig. 1.

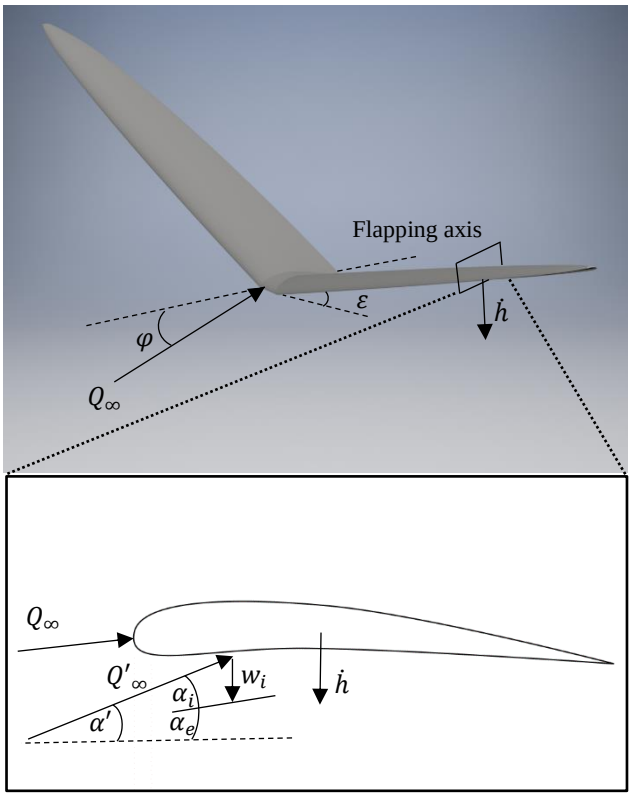

Fig. 1. The absolute and relative flow angles experienced by flapping wing airfoil

According to Polhamus' suction analogy, during dynamic stall the suction force rotates 90 degrees and acts perpendicular to the wing cord rather than parallel, forming an LEV [7]. Lift of the wing sections in dynamic stall is given by Eq. 7, where suction force and its coefficient for a 2-D airfoil are provided by Eqs. 8 and 9, respectively [8].

$$L_{DS} = 2\rho \int_{y_{Attached}}^{\frac{b}{2}} Q'_\infty \cos(\varepsilon)\cos(\varphi+\gamma)\Gamma\, dy + 2\int_{y_{Attached}}^{b/2} \cos(\varepsilon)\,(\cos(\varphi+\gamma) - \sin(\varphi+\gamma))\, dF_s \quad (7)$$

where

$$\alpha' \leq (\alpha_{attached})_{min} \quad or \quad \alpha' \geq (\alpha_{attached})_{max}$$

$$dF_s = \frac{1}{2}\rho c C_s {Q'_\infty}^2 dy \quad (8)$$

$$C_s = 2\pi n_s {\alpha_e}^2 \quad (9)$$

2π is the theoretical maximum local lift slope of an airfoil as stated by the thin airfoil theory. Thus, 2π can be replaced by m the local 2-D lift slope of the airfoil as shown in Eq. 10. Based on traditional lifting line theory the effective angle of attack α_e is given by Eq. 11. Substituting Eqs. 10 and 11 into Eq. 8 yields the simplified form of Eq. 12.

$$C_s = m n_s {\alpha_e}^2 \quad (10)$$

$$\alpha_e = \frac{2\Gamma}{mcQ'_\infty} \quad (11)$$

$$dF_s = \frac{2\rho {n_s}^2}{mc}(\Gamma)^2 dy \quad (12)$$

Total drag is calculated through Eq. 13, which is the sum of induced drag and viscous drag. Even though viscous drag is accounted for in this model, it is usually small and may be approximated as zero for noncritical estimates. Eq. 14 gives the induced drag acting on the wing. The second term in the equation accounts for the rotation of the suction force over the dynamically stalled portion of the wing. Induced drag is dependent on induced downwash angle given by Eq. 15, with viscous drag force represented in Eq. 16. The viscous drag coefficient C_{df} can be determined numerically, but likely will be underestimate. For better estimation, skin roughness C_{df} should be determined from experimentation such as a wind tunnel test. When thrust is being produced D_{Total} becomes negative.

$$D_{Total} = D_i + D_f \quad (13)$$

$$D_i = \rho \int_{-\frac{b}{2}}^{\frac{b}{2}} Q'_\infty \cos(\varphi+\gamma)\sin(\alpha'_i)\,\Gamma\, dy + 2\int_{y_{Attached}}^{b/2} -\cos(\varphi+\gamma) - \sin(\varphi+\gamma)\,\mathrm{dF}_s \quad (14)$$

$$\alpha'_i = \alpha' - \frac{2\Gamma}{mcQ'_\infty} - \alpha_{L0} \quad (15)$$

$$D_f = \frac{1}{2}\rho \int_{-b/2}^{b} C_{df}(Q'_\infty \cos(\alpha'))^2\, dy \quad (16)$$

The circulation used in the previous equations can be found by solving the lifting line integro-differential Eq. 17.

$$\frac{-2\Gamma}{mcQ'_\infty} - \frac{1}{4\pi Q'_\infty}\int_{-\frac{b}{2}}^{\frac{b}{2}} \frac{[\mathrm{d}\Gamma(y_0)/dy]dy_0}{y-y_0} + \alpha' - \alpha_{L0} = 0 \quad (17)$$

The circulation can be described by a Fourier expansion as shown in Eq. 18. For Fourier series, the span wise coordinate must be changed from y to θ, whereby $y = \frac{-b}{2}$ is equivalent to $\theta = \pi$ and $y = \frac{b}{2}$ is equivalent to $\theta = 0$. The relationship between y and θ is shown in Eq. 19.

$$\Gamma = 2b\sum_{n=1}^{\infty} A_n \sin(n\theta) \quad (18)$$

$$y = \frac{b}{2}\cos(\theta) \quad (19)$$

Substituting Eq. 18 into Eq. 17 yields Eq. 20. The second term can be simplified using Glauert's integral resulting in Eq. 21. The condensed form can be shown in the form of Eq. 22.

$$0 = \frac{-4b}{mcQ'_\infty}\sum_{n=1}^{\infty} A_n \sin(n\theta) - \frac{1}{\pi Q'_\infty}\int_0^\pi \frac{\sum_{n=1}^{\infty} nA_n \cos(n\theta_0)\, d\theta_0}{\cos(\theta_0)-\cos(\theta)} + \alpha' - \alpha_{L0} \quad (20)$$

$$0 = \frac{-4b}{mcQ'_\infty}\sum_{n=1}^{\infty} A_n \sin(n\theta) - \frac{1}{Q'_\infty}\sum_{n=1}^{\infty} nA_n \frac{\sin(n\theta)}{\sin(\theta)} + \alpha' - \alpha_{L0} \quad (21)$$

$$\sum_{n=1}^{\infty} A_n \sin(n\theta)\left(\frac{4b}{mc} + \frac{n}{\sin(\theta)}\right) = Q'_\infty(\alpha' - \alpha_{L0}) \quad (22)$$

An analytical solution to the above equation can be found for an elliptical wing with a uniform lift slope in which $c = c_{max}\sin(\theta)$, where c_{max} is the chord length at the root of the semi-span. This results in Eq. 23. As the right hand side of the equation is a Fourier expansion, the coefficients A_n can be found using Eq. 24.

$$\sum_{n=1}^{\infty} A_n \sin(n\theta)\left(\frac{4b+nmc_{max}}{mc_{max}}\right) = Q'_\infty(\alpha' - \alpha_{L0})\sin(\theta) \quad (23)$$

$$A_n = \frac{2mc_{max}}{\pi(4b+nmc_{max})} \times \int_0^{\pi} Q'_{\infty}(\alpha' - \alpha_{L0})\sin(\theta)\sin(n\theta)d\theta \quad (24)$$

4 Model Comparison With Experimental Results

In order to access the accuracy of the above modeling approach, results from the model have been compared to experimental results from the literature. The experimental study used examines the lift generated by a flapping goose model that was placed within a wind tunnel [3]. The model had a single degree of freedom flapping motion and was tested at several different Reynolds numbers (Re), and frequencies [3]. The wing of the model was not exactly elliptical, but was deemed close enough to provide a preliminary validation. Experimental curves in Fig. 2-4 taken from [3]

Fig. 2 shows the first case. There is generally good agreement between maximum and minimum experimental and predicted coefficient of lift produced by the wing. There is also a slight time offset between the predicted point and experimental point of maximum lift. This is also the case for the other comparisons. Such an offset is expected and normally caused by unsteady effects, which will be accounted for in future iterations of the model.

For the first case, relative angle of attack was small enough (less than 10°), whereby dynamic stall was predicted to not have occurred.

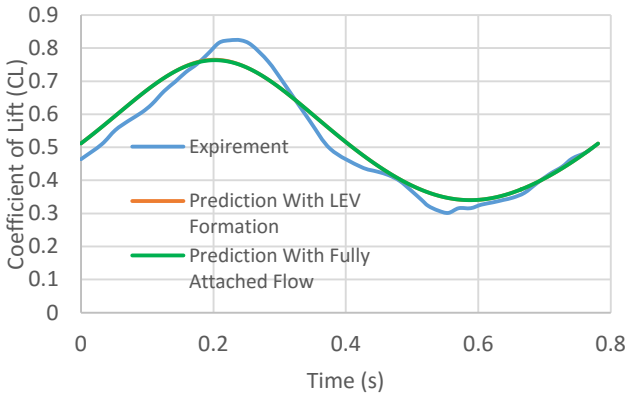

Fig. 2. Flapping wing with a Re of 113000 and a flapping frequency of 1.28 Hz

For the second case, shown in Fig. 3, the frequency was higher (2.02 Hz vs 1.28 Hz), leading to a higher angle of attack. In this case dynamic stall was shown to have occurred.

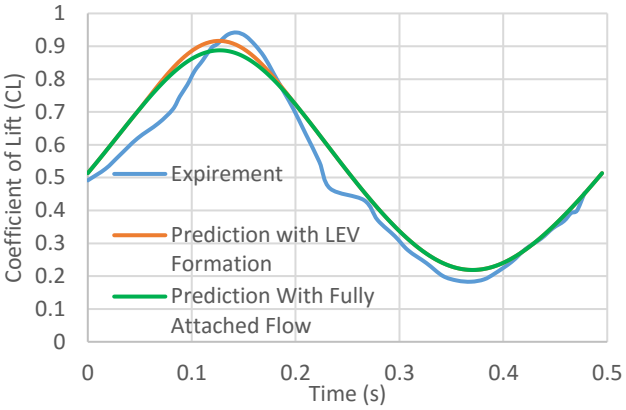

Fig. 3. Flapping wing with a Re of 113000 and a flapping frequency of 2.02 Hz

For the last case shown in Fig. 4, the model overestimates the maximum lift produced. The main reason for this seems to be the fact that Re for this case was half of that of the previous two cases. The 2-D airfoil data documented in the literature and used for the predictions was at a Re of 100,000. At a Re of 56,000 the airfoil lift slope and stall angles may have decreased. In fact, this is very likely as even low Re airfoils do not operate as efficiently in this Re range.

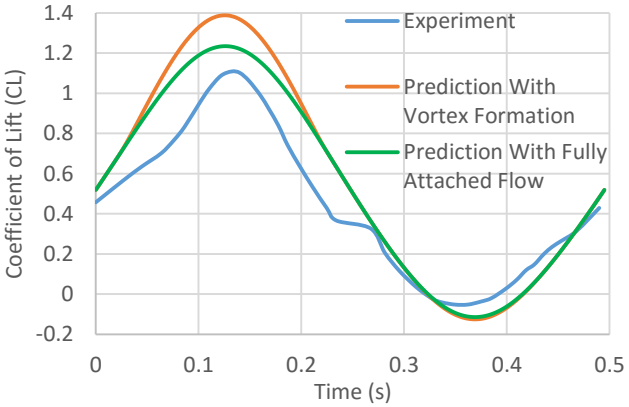

Fig. 4. Flapping wing with a Re of 113000 and a flapping frequency of 2.02 Hz

The proposed model's LEV prediction appears to partially match with experimental results. Experimental cases 2 and 3, shown in Figs. 3 and 4, illustrate a significant change in lift slope at approximately 0.8 and 0.7 seconds respectively suggesting the formation of an LEV. The model

predicts the LEV formation for both of these cases as well, though the transition in the model is smoother. For the first experimental case, shown in Fig. 2, there is no drastic change in lift slope suggesting the wing does not reach dynamic stall. This is also predicted by the model.

The proposed model exhibits a potential to be a good predictor of lift generation for a flapping wing, but it is yet be confirmed. While the geometry and kinematics of the wing used in the experiment are well defined, whether the wing exactly followed the prescribed kinematics was not well documented. Furthermore, the unreported rigidity of the wing and the subsequent aero-elastic effects may have played a role.

5 Future Comparison With Lattice Boltzman Method

In order to better validate this approach, predictions from the model will be compared with higher order CFD results. Using CFD rather than experimental data allows for more precise control of kinematics and geometry as well as allows for removal of error inducing external factors such wall effects. The CFD method of choice utilizes the Lattice Boltzmann Method (LBM) with adaptive mesh refinement. The reason LBM was chosen is because of its decreased computation time and ability to capture vortex structures relatively better than traditional Navier-Stokes based methods [9]. Fig. 5 provides an example of preliminary results of an elliptical bird like flapping wing.

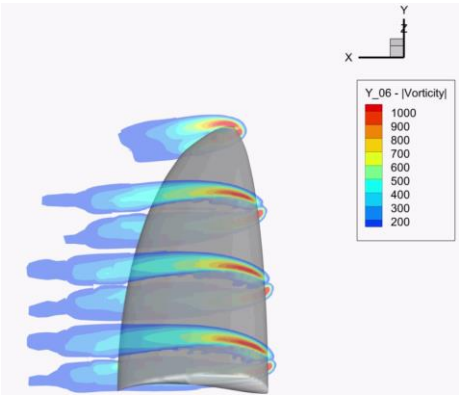

Fig. 5. Elliptical flapping wing with 0.7 meter semi-span and s1223 airfoil

6 Conclusion

In conclusion, a modified lifting line model for bird like flapping wings was developed. This lifting line model is unique in that it accounts for LEV formation. The current version of the model shows good agreement with experimental results. Future work includes developing the model to better account for delay in lift generation due to unsteady effects, and more in depth validation using LBM.

Acknowledgements

The authors would like to thank Professor Jae-Hung Han and the Smart Systems and Structures Lab at KAIST for their valuable input during the course of this study. Also, Jeffery Feaster's (a member of *CRASH* Lab) assistance with the LBM is greatly acknowledged.

References

[1] Hoa S, Nassefa H, Pornsinsirirak N, et al. Unsteady aerodynamics and flow control for flapping flyers. *Progress in Aerospace Sciences*, Vol. 39, No. 8, pp. 635-681, 2003

[2] Philips W. Analytical Decomposition of Wing Roll and Flapping Using Lifting-Line Theory. *Journal of Aircraft*, Vol .51, No. 3, pp.761-778, 2014

[3] Hubel T, Tropea C. Experimental investigation of a flapping wing model. *Experiments in Fluids*, Vol. 46, No. 5, pp. 945-961, 2008

[4] Kim D, Lee J, Han J. Improved Aerodynamic Model for Efficient Analysis of Flapping-Wing Flight. *AIAA Journal*, Vol. 49, No. 4, pp.868-872, 2011

[5] Lui T, Kuykendoll K, Rhew R, and Jones S. Avian Wing Geometry and Kinematics. *AIAA Journal*, Vol. 44, No. 5, pp. 954-963, 2006

[6] Delaurier J. An aerodynamic model for flapping-wing flight. *The Aeronautical Journal of the Royal Aeronautical Society*, pp. 125-130, 1993

[7] Polhamus E. Predictions of Vortex-Lift Characteristics by Leading-Edge Suction Analogy. *Journal of Aircraft*, Vol. 8, No. 4, pp. 193-199, 1971

[8] Delaurier J. Drag of Wings with Cambered Airfoils and Partial Leading-Edge Suction. *Journal of Aircraft*, Vol. 20, No. 10, pp. 882-886, 1983

[9] Feaster J, Battaglia F, Deiterding R, and Bayandor J. Validation of an adaptive meshing implementation of the Lattice-Boltzman Method for insect flight. *Proceedings of the ASME Fluids Engineering Division Summer Meeting*, Washington DC, FEDSM2016-7782, pp. 1-7, 2016

Contact Author Email Address

mailto: amatta@vt.edu
bayandor@vt.edu

Copyright Statement